

Specific Polarizability of Sand-Clay Mixtures with Varying Ethanol Concentration

by

Sundeeep Sharma

A Dissertation submitted to the

Graduate School-Newark

Rutgers, The State University of New Jersey

In partial fulfillment of the requirements

for the degree of

Master of Science

Graduate Program in Environmental Geology

written under the direction of

Lee D. Slater

and approved by

Newark, New Jersey

January, 2016

Copyright page:

©2015

Sundeep Sharma

ALL RIGHTS RESERVED

ABSTRACT OF DISSERTATION

Specific Polarizability of Sand-Clay Mixtures with Varying Ethanol Concentration

By Sundeep Sharma

Dissertation Director:

Dr. Lee D. Slater

I utilize the concept of specific polarizability (c_s), represented as the ratio of mineral-fluid interface polarization per pore-normalized surface area S_p , to emphasize the influence of clay mineralogy and fluid chemistry on complex conductivity (CC) measurements. CC measurements were performed on kaolinite- and illite- sand mixtures as a function of varying ethanol (EtOH) concentration (10% and 20% v/v). Specific surface area of each clay type and Ottawa sand was determined by nitrogen gas adsorption-BET method. I also calculated porosity and saturation of each mixture based on weight loss of dried samples. Debye decomposition, a phenomenological model, was applied to the CC data to determine normalized chargeability (m_n). The c_s estimates from previous CC measurements for bentonite-sand mixtures were compared with our dataset. The c_s for all sand-clay mixtures decreased as the EtOH concentration increased from 0% to 10% to 20%. We observe similar responses to clay-driven polarization for all sand-clay mixtures. Analysis of variance (ANOVA) with a level of significance $\alpha = 0.05$ found that suppression in c_s responses with increasing EtOH concentration statistically vary for all sand-clay mixtures but the confidence level for c_s is low. On the other hand, real conductivity showed only small changes with increasing EtOH concentration from 10%

to 20%. The c_s estimates reflect the sensitivity of CC measurements to alteration in surface chemistry at the available surface adsorption sites (internal and external) for different clay types assumed to result from chemical ion exchange at clay surface and kinetic reactions in the electrical double layer of the clay-water-EtOH media.

Acknowledgements

First and foremost, I would like to sincerely thank my advisor, Dr. Lee Slater, for his continued support and his encouraging presence from the beginning of my graduate career until the achievement of my thesis. I am also equally grateful to my thesis committee members, Dimitrios Ntarlagiannis (Rutgers), Dale Werkema (USEPA) and Zoltan Szabo (Rutgers/USGS), for providing valuable support every step of the way. It was not only a privilege but an honor to work with such esteemed researchers.

I would also like to thank the faculty and staff at the Department of Earth and Environmental Sciences. In particular, I would like to thank Liz Morrin for her continued assistance in finishing all the necessary paperwork, class enrollment and other administrative tasks. I also thank Dr. Yves Personna for allowing us to use his data for comparison in our paper, and his constructive reviews on my work. I would also like to thank Sweeta Chauhan for her encouragement every step of the way.

I am also thankful for my fellow graduate students and friends at this department. I would personally like to thank Jeffery Heenan, Casey McGuffy, Jung Yun and Jan Olechowski for their help with the lab work. Without their help, my thesis would not have been possible.

I would also like to thank Dr. Estella Atkewana (Oklahoma State University) and Carl Rosier (Oklahoma State University) for their assistance with my paper. I would also like to sincerely thank Allison Enright (University of Toronto) for all her support and critical reviews of my thesis defense presentation.

I would also like to acknowledge the financial support of the United States Environmental Protection Agency through its Office of Research and Development under contract #EP-13-D-000143 to Sundeep Sharma.

Last but not the least, I would like to thank my parents and family for all their support. Without them, I would not have achieved so much in life. A big thank you to my mother, Lata Sharma, for the unconditional love she has provided since the day I entered this world. I would also like to thank my father, Dr. Krishan Sharma, who always inspired me to thrive for success by being an incredible mentor and a loving father. A special thanks to Nicole Paizis for her support through my work.

Table of Contents

ABSTRACT OF THE DISSERTATION	iii
ACKNOWLEDGEMENTS	v
TABLE OF CONTENTS	vii
LIST OF TABLES	viii
LIST OF ILLUSTRATIONS.....	ix
INTRODUCTION.....	1
CLAY MINERALS.....	6
ELECTRICAL PROPERTIES.....	9
COMPLEX CONDUCTIVITY MODELING.....	11
INFLUENCE OF SALINITY AND MINERALOGY ON COMPLEX CONDUCTIVITY RESPONSES.....	12
INFLUENCE OF SAMPLE SATURATION AND CLAY CONTENT ON IMAGINARY CONDUCTIVITY.....	17
METHODS.....	19
RESULTS.....	24
DISCUSSION.....	27
CONCLUSIONS.....	31
REFERENCES.....	33
APPENDIX.....	39

List of Tables

Table 1 – Summary of the physical properties of clays and sand-clay mixtures.

Table 2 – Percentage change (%) in c_p , c_s , real and imaginary conductivity. Imaginary conductivity show is for 1 Hz frequency. Negative and positive values indicate decrease or increase in c_p / c_s / real conductivity / imaginary conductivity relative to 10% EtOH sample, respectively.

List of Illustrations

Figure 1 – Phase response for clayey (montmorillonite) soil samples with varying toluene concentration in the pore-filling fluid. Open symbols are laboratory mixture of montmorillonite with 20% w/w toluene and 0.001 molar KCl solution (modified from Olhoeft 1992)

Figure 2 - CC response of sample containing 5% montmorillonite as a function of toluene concentration at late time; a) relative change in imaginary (open symbols) and real (solid symbols) conductivity; b) phase response at varying toluene concentration. Symbols represent measured data and solid lines are values from Debye Decomposition fit.

Figure 3 – Phase (ϕ) and imaginary conductivity (σ'') responses for 2% w/w bentonite mixture as a function of increasing ethanol concentration (v/v).

Figure 4 – Structural patterns for 1:1 and 2:1 clays. The kaolinite structure is stacked by hydrogen bonding, resulting in no interlayer spaces between two sheets. In illite, the interlayer space is occupied by potassium cations. In bentonite, the interlayer spaces are occupied by water and common substitutes such as sodium, magnesium and calcium cations.

Figure 5 - Imaginary conductivity (σ'') and pore-normalized specific surface area (S_p) relation observed by Weller et al. (2010) for an extensive database of 114 samples.

Figure 6 – Normalized chargeability (m_n) and pore-normalized specific surface area (S_p) relation observed by Weller et al. (2010) for an extensive database of 114 samples.

Figure 7 – Relationship between S_p (BET and MB estimates) and imaginary conductivity (σ'') observed by Weller et al. (2015).

Figure 8 – Imaginary conductivity spectra as a function of saturation; a) during evaporative drying, b) during pressure drainage (Ulrich and Slater 2004).

Figure 9 – Imaginary conductivity vs. percent saturation degree shows a power law relationship (Grunat et al., 2013).

Figure 10 – Plot of real and imaginary conductivity of clay-sand mixtures. K2 represents kaolinite and B2 represent bentonite. The samples were saturated with distilled water (Okay et al., 2014).

Figure 11 – Experimental setup schematic showing the sample holders constructed using cylindrical transparent PVC (inner diameter = 0.025m and length = 0.028 m). The location of two coiled Ag-AgCl current electrodes (C_1 and C_2) and two Ag-AgCl potential electrodes (P_1 and P_2) are shown.

Figure 12 – Summary of experimental treatment applied to samples. We applied three experimental treatments to our samples saturated with either KCl (0% EtOH) or KCl

containing 10% or 20% EtOH (v/v). Personna et al. (2013) applied a similar experimental treatment to the bentonite clay sample, with EtOH blank being water instead of KCl.

Figure 13 – Specific polarizability (c_p) responses for different clay minerals: a) bentonite (blue), b) illite (red) c) kaolinite (black) and d) Ottawa sand as a function of ethanol concentration (v/v) (EtOH 0%, EtOH 10% and EtOH 20%).

Figure 14 – Temporal variation in specific polarizability (c_p) response for Ottawa sand sample with 10% EtOH.

Figure 15 – Plot of specific polarizability (c_s) versus measured EtOH concentration for different sand-clay mixtures.

Appendix A1 – Specific polarizability (C_p) of 2% kaolinite-98% sand mixture with varying ethanol concentration

Appendix A2– Specific polarizability (C_p) for 4% kaolinite-96% sand mixture with varying ethanol concentration.

Appendix A3 – Specific polarizability (C_p) spectra for 2% and 4%- kaolinite mixture with varying ethanol concentration.

Introduction

Ethanol is now widely used as an additive to conventional fuel to provide cleaner emissions during internal combustion in various automotive engines. Ethanol enters groundwater reserves in the subsurface through accidental spills and it has now emerged as a leading contaminant in groundwater (Gomez and Alvarez, 2010). Powers et al. (2001a) describe the potential risks to groundwater due to accidental spills of large volumes of gasoline containing ethanol during transportation. Increased concentrations of ethanol in ground water also result in slower degradation of the BTEX (benzene, toluene, ethyl-benzene and xylene) compounds present in gasoline. In groundwater containing ethanol and BTEX compounds, ethanol is preferentially biodegraded by microbes over BTEX compounds (Corseuil et al., 1998; Powers et al., 2001b; Lovanh et al., 2002; Ruiz-Aguilar et al., 2002; Österreicher-Cunha et al., 2007; Schaefer et al., 2010), resulting in rapid depletion of dissolved oxygen and other essential electron acceptors required for BTEX biodegradation.

Determining the location of subsurface contaminant plumes in porous media is essential for designing successful bioremediation processes. Non-invasive geophysical techniques may help delineate organic contaminant plumes in the subsurface. Olhoeft (1985), Olhoeft (1986) and Sadowski (1988) first suggested the potential of low frequency electrical methods for delineating regions associated with clay-organic interactions in the subsurface. In particular, Olhoeft (1985) carried out the first study on detecting organic contamination using conductivity (CC). In this early study, montmorillonite samples were

saturated using pore fluid with and without toluene and the CC of the resultant interaction was measured. Figure 1 shows the main result of Olhoeft (1985). The curves with solids symbol represent measurements done on samples from a landfill site and open symbols represent measurements on a laboratory mixture of SWy-1 montmorillonite with 20 weight percent toluene with 0.001 molar KCl solution reported by Sadowski (1988). The resultant increase in phase (up to ~ 100 mrad) with increase in toluene concentration was interpreted as the enhancement in surface polarization due to adsorption of organic cations onto clay surfaces. This change in phase (ϕ) as result of clay-organic reactions prompted further research into electrical signatures of organic contaminants (Olhoeft, 1985; Sadowski, 1988; Olhoeft and King, 1991).

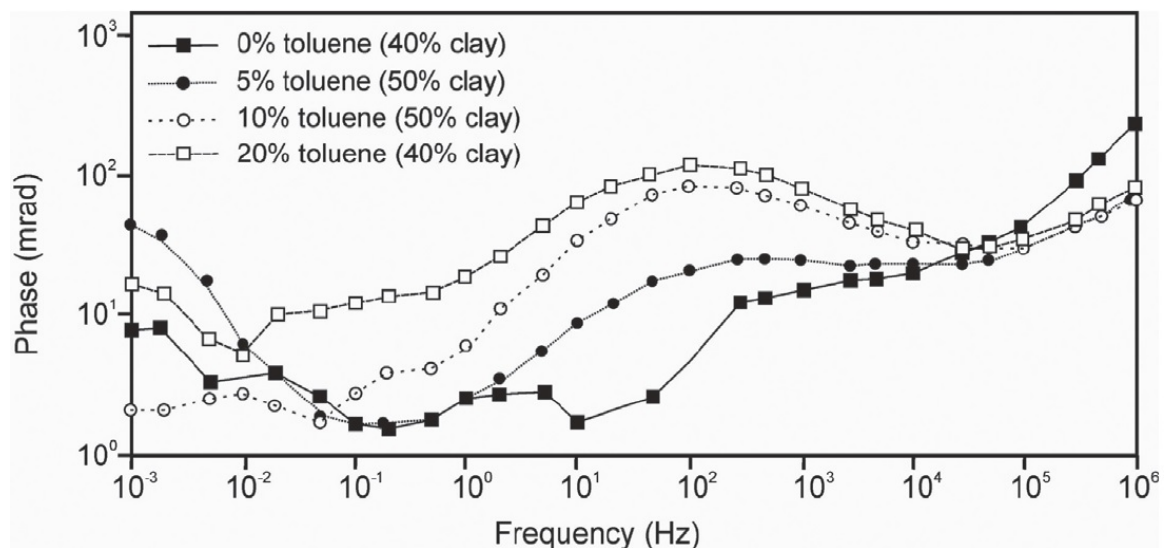


Figure 1- Phase (ϕ) response for clayey (montmorillonite) soil samples with varying toluene concentration in the pore-filling fluid. The fluid samples were made by adding specific percentage of toluene in a 0.001 molar KCl solution (modified from Olhoeft 1992).

However, later efforts by Brown et al. (2004) were unsuccessful in reproducing ϕ responses associated with clay-toluene interactions reported by Olhoeft (1985). Such inconsistent findings encouraged further research to determine the geoelectric responses associated with clay-organic interactions. Figure 2 shows results from a study by Ustra et.al (2012) which demonstrated a time dependence of CC measurements for clayey soil samples containing toluene. They noted a smaller, yet significant, effect of toluene content on the phase response, shortly after sample preparation, followed by no significant relation between CC measurements and toluene content at electrical equilibrium after 40 days. Contrary to Olhoeft (1985), Ustra et.al (2012) found that the presence of toluene shortly after sample preparation suppressed (rather than enhanced) the CC response.

Personna et al. (2013) performed a series of laboratory experiments on sand-clay mixtures with varying concentrations of ethanol. Figure 3 shows the phase (ϕ) and imaginary conductivity (σ'') for sand with 2% bentonite as a function of increasing ethanol concentration observed by Personna et al. (2013). Again, contrary to earlier studies by Olhoeft and colleagues on CC measurements of clay-organic interaction, Personna et al. (2013) observed a clear decrease in measured phase and imaginary part of complex conductivity for a sand-bentonite matrix with increasing concentration of ethanol in the pore-filling fluid. The magnitude of this decrease increased with increased ethanol concentration in the ethanol-water mixtures. Personna et al. (2013) attributed this behavior to a variety of possible scenarios at the mineral-fluid interface, such as cation-dipole interactions resulting in preferential and strong adsorption of EtOH relative to water on clay surfaces.

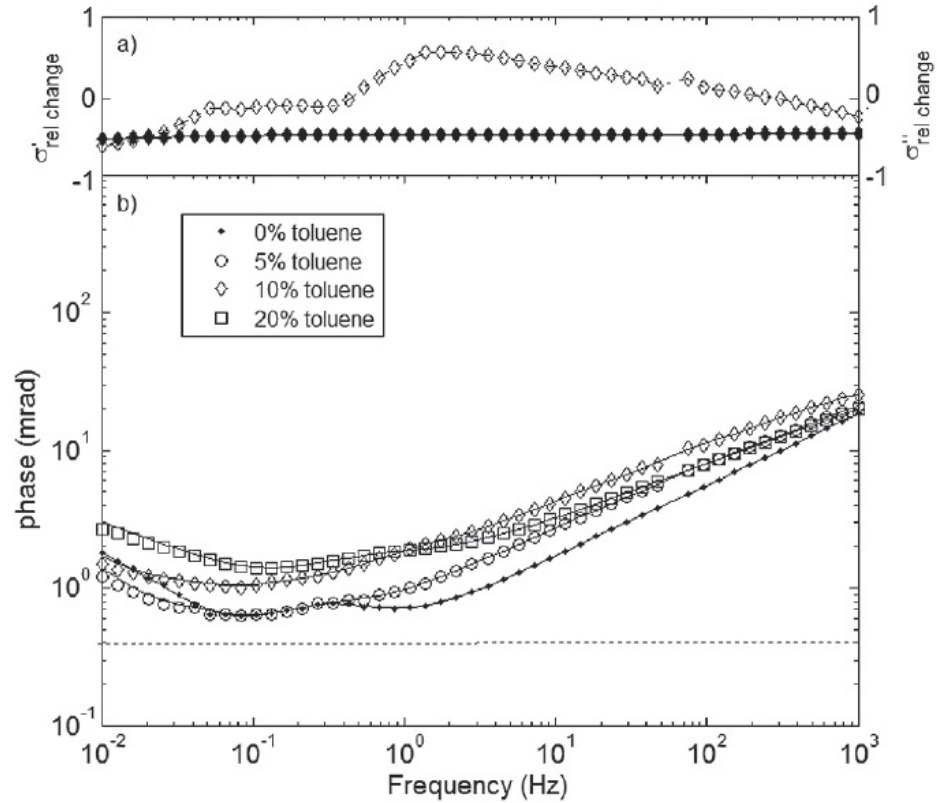


Figure 2 - CC response of a sample containing 5% montmorillonite as a function of toluene concentration at electrical equilibrium; a) relative change in imaginary (open symbols) and real (solid symbols) conductivity; b) phase response at varying toluene concentration. Symbols represent measured data and solid lines are values from Debye Decomposition fit (Ustra et al., 2012)

The concept of specific polarizability (c_p and c_s) has been documented in several key literatures in the last decade. This concept is based on normalizing the imaginary conductivity by the pore normalized surface area (S_p) and represents the control of fluid chemistry and/or mineralogy on the CC measurements (Weller et al., 2010; Weller et al., 2011; Weller et al., 2015).

The purpose of this study is to better understand the effect of mineralogy and changes in pore-fluid chemistry on the CC signatures of different sand-clay mixtures. We apply the concept of c_p to our CC data for different sand-clay mixtures. Variations in the c_p for different clay types were expected to result from the difference in mineralogy for different types of clays used in our mixtures and/or the varying EtOH concentration in the pore-filling fluid. Our main objective was to determine the c_p variation associated with the interaction of EtOH with different clay types with varying specific surface area and adsorption capacity. We explore c_p variation resulting from changes in the mineralogy between kaolinite (1:1) clay and illite (2:1) clay and its subsequent interaction with EtOH. We compare the variations in c_p from our samples with c_p calculated for bentonite (2:1) clay mixture measured by Personna et al (2013).

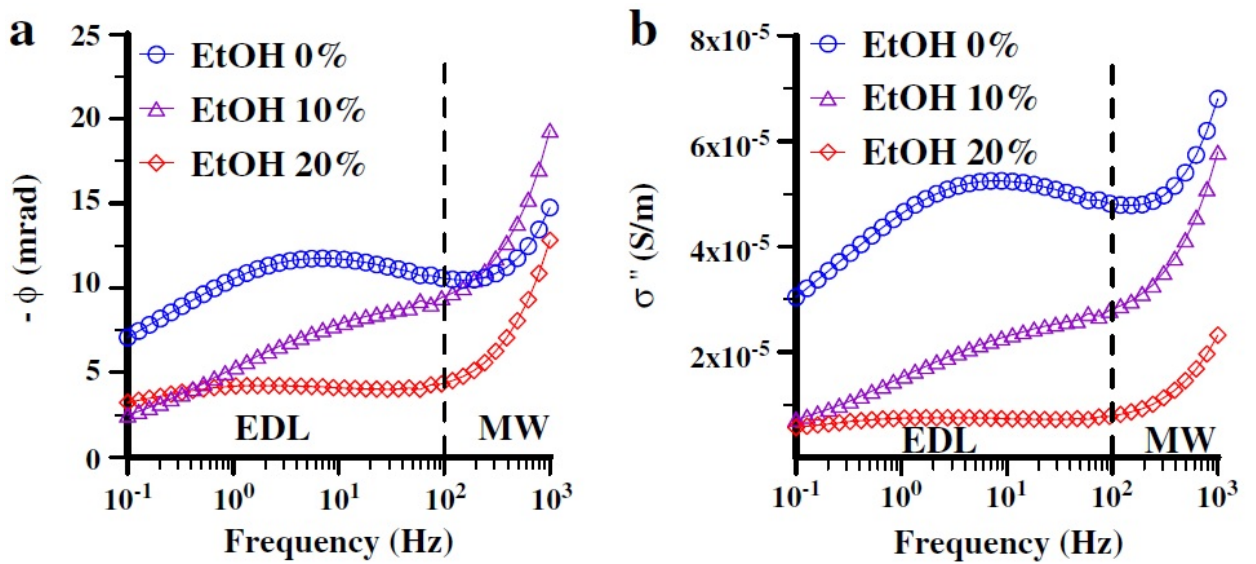


Figure 3 - Phase (ϕ) and imaginary conductivity (σ'') responses for 2% w/w bentonite mixture as a function of increasing ethanol concentration (v/v) (Personna et al., 2013)

Clay Minerals

Under natural groundwater conditions, a clay mineral generally carries a fixed net negative charge on the surface due to changes in total net charge resulting from isomorphic substitution by elements of similar size and lower valence. This negative charge is fulfilled by adsorption of cations on the surface of the clay mineral (VanOlphen, 1997; Sposito et al., 1999). In 2:1 clay minerals, such as montmorillonite, illite, or bentonite, there are two tetrahedral sheets on each side of an octahedral sheet (T-O-T) and water molecules can be readily adsorbed onto the exchangeable cations (Figure 4). In contrast, a 1:1 clay mineral, such as kaolinite, is characterized by an alternating two-sheet layer structure composed of one silica tetrahedral sheet and one alumina octahedral sheet (Spagnoli et al. 2010). As a result of chemical bonding between the silica and alumina sheets, the inner hydroxyl plane in 1:1 clay is inaccessible for ion interactions. For such clay types, only the outer groups, located along the unshared plane, are available for interactions with ions and organic molecules (Miranda & Coles, 2003).

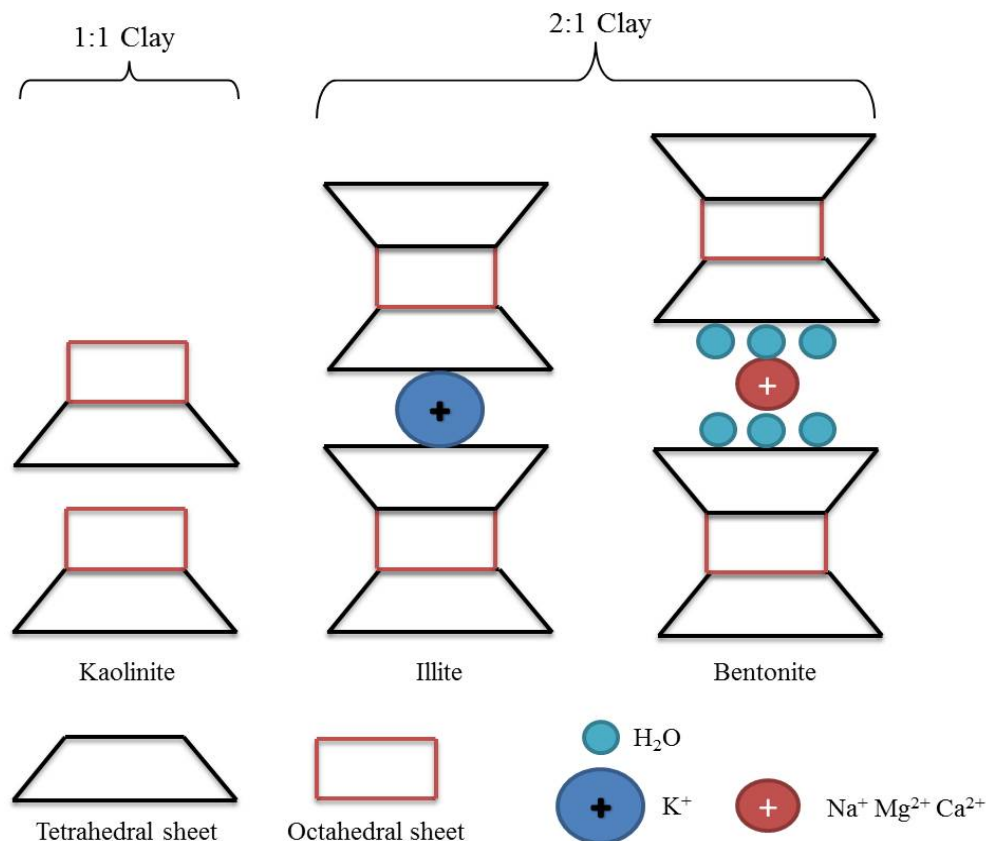


Figure 4 - Structural patterns for 1:1 and 2:1 clays. The kaolinite structure is stacked by hydrogen bonding, resulting in no interlayer spaces between two sheets. In illite, the interlayer space is occupied by potassium cations. In bentonite, the interlayer spaces are occupied by water and common substitutes such as sodium, magnesium and calcium cations (modified from Craig, 1947).

The electrical double layer (EDL) model is commonly used to describe the electric charge distribution at the mineral/water interface. The EDL consists of (a) a Stern layer formed as a result of direct ion sorption on the mineral surface, and (b) a diffuse layer which consists of mostly freely moving excess counter ions extending beyond the Stern layer (Revil et al.,2012). Saidy et al. (2012) showed an increase in the adsorption capacity

for dissolved organic compounds onto clay in the order kaolinite < illite < montmorillonite. In 2:1 clay minerals, EtOH molecules, like water molecules, can be adsorbed onto the inner surface. Dowdy & Mortland (1967) and German & Harding (1969) demonstrated the affinity of EtOH and other alcohols for these adsorption sites between clay sheets. EtOH has been shown to be capable of replacing water in 2:1 clays in the inner hydration shell around cations such as Ca^{2+} , Cu^{2+} and Al^{3+} . Parke & Birch (1999) and Atamas & Atamas (2009) describe how the competition of EtOH for adsorption on available cation sites in a clay structure leads to complex intermolecular interactions. These interactions at the mineral-fluid interface can extensively alter mobility of ions in solution (Bhatt and Shetty, 2011). They therefore also have the potential to change interfacial electrical properties measured with CC as considered here.

Okay et al. (2014) studied the effect of clay content and clay mineralogy on the CC response in a well-controlled laboratory experiment with water-saturated unconsolidated clays and sand-clay mixtures. They analyzed two classes of samples, where K1 and K2 were kaolinite samples and B1 and B2 were bentonite samples. Different weight fractions of kaolinite and bentonite samples were mixed with Fontainebleau sand (99.98% silica-pure sand) to prepare various mixtures. We only show CC data for K2 (95%/w kaolin, $S_s = 9.4 \text{ m}^2/\text{g}$) and B2 (95%/w smectite, $S_s = 27 \text{ m}^2/\text{g}$) clay mixtures in sand (Figure 10).

Okay et al. (2014) observe generally higher imaginary conductivities for bentonite-sand samples as compared to kaolinite-sand samples. Okay et al. (2014) attribute this behavior to higher cation exchange capacity (CEC) for bentonite ($\text{CEC}_{\text{kaolinite}} = < 0.10 \text{ meq g}^{-1}$, $\text{CEC}_{\text{bentonite}} = 0.44 \text{ meq g}^{-1}$) as compare to kaolinite.

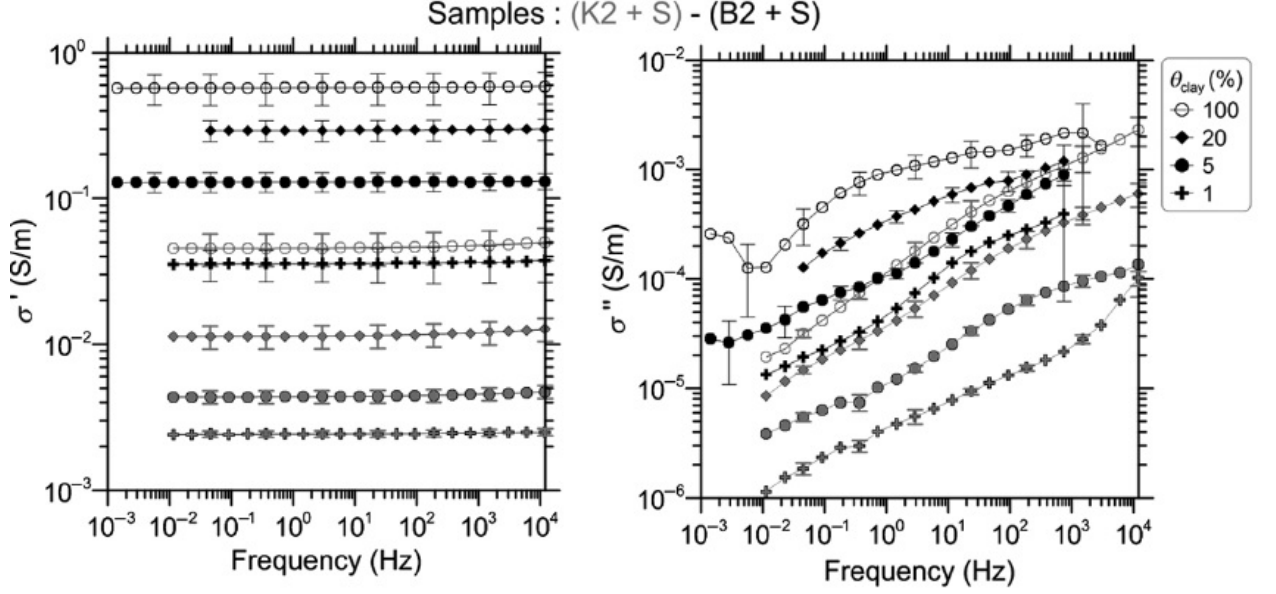


Figure 5 - Plot of real and imaginary conductivity of clay-sand mixtures. K2 represents kaolinite and B2 represent bentonite. The samples were saturated with distilled water (Okay et al., 2014).

Electrical Properties

The CC method characterizes the capacitive and conductive properties of a material over a range of frequencies (typically 0.001 to 1000 Hz). In geophysical applications, the measured electrical properties are often represented by the conductivity magnitude ($|\sigma|$) and phase shift (ϕ) of the measured voltage waveform across a sample relative to the current waveform measured across a resistor placed in series.

$$|\sigma| = \sqrt{(\sigma')^2 + (\sigma'')^2}, \quad (1)$$

$$\phi = \tan^{-1}(\sigma''/\sigma'), \quad (2)$$

where σ' represents the real part and σ'' represents the imaginary part of the CC (σ^*).

These measurements can be represented in terms of real (in phase) and imaginary (out of phase) components of the complex conductivity σ^* by,

$$\sigma' = |\sigma| \cos \phi, \quad (3)$$

$$\sigma'' = |\sigma| \sin \phi. \quad (4)$$

In a non-metallic porous medium, electrical conduction can follow two paths, a) electrolytic conduction through fluid filled interconnected pore spaces, and (b) surface conduction within the electrical double layer. The electrolytic and surface conductivities are generally assumed to add in parallel (Waxman and Smits, 1968; Lesmes and Frye, 2001). With this assumption, σ' and σ'' are expressed in terms of fluid conductivity (σ_w) and surface conductivity (σ''_{surf}) by:

$$\sigma' = \frac{1}{F} \sigma_w + \sigma'_{surf}, \quad (5)$$

$$\sigma'' = \sigma''_{surf} \quad (6)$$

where F represents the formation factor, being the ratio of conductivity of the saturating fluid to the conductivity of the fluid-saturated porous media (Archie, 1942). The imaginary part (σ'') of complex conductivity is a direct measure of the interfacial properties (equation 6) and is therefore sensitive to changes in surface electrochemistry.

Complex conductivity modeling

Mechanisms that generate CC responses in soils are not yet entirely understood. The surface conductivity is a result of electrochemical processes governed by the chemical and physical characteristics of soils. The interpretation of the CC signature associated with clay-EtOH-water mixtures is challenging. There is currently no physicochemical model that can describe such interactions. Instead, phenomenological models such as the Cole-Cole relaxation models can be used to empirically describe the CC dependence on physical and chemical properties of soils (Cole and Cole, 1941; Davidson and Cole, 1951). The generalized Cole-Cole model can be expressed in terms of CC as

$$\rho(\omega) = \rho_0 \left[1 - m \left(1 - \frac{1}{(1 + (i\omega\tau)^c)^a} \right) \right] \quad (6)$$

where ρ_0 is the DC resistivity, τ is the time constant, m is the chargeability and c and a are constants that describe dispersion shape observed in CC data (Pelton et al., 1978).

Similarly, the Debye decomposition (DD) procedure can be used to describe the CC spectra in terms of a smaller number of quantifiable parameters (Lesmes and Morgan, 2001; Nordsiek and Weller, 2008). As compared to Cole-Cole type models, the DD method fits a wider range of shapes of phase spectra (Nordsiek and Weller 2008).

According to Nordsiek and Weller (2008),

$$\rho(\omega) = \rho_0 \left[1 - \sum_{k=1}^n m_k \left(1 - \frac{1}{1 + i\omega\tau_k} \right) \right] \quad (7)$$

where n is the number of individual Debye responses. This approach relies on decomposition of the CC spectra into n discrete Debye responses with specific

chargeability (m_k) and relaxation time (τ_k) (for more details, refer to Zisser et al., 2010 and Norsiek and Weller 2008). The integral or total chargeability (m) is then obtained by,

$$m = \sum_{k=1}^n m_k \quad (8)$$

To obtain a global direct estimate of the polarizability of the material over the measured frequency range, normalized chargeability can be obtained as such (Lesmes and Frye, 2001; Slater and Lesmes, 2002),

$$m_n = m\sigma_0 \quad (9)$$

Influence of salinity and mineralogy on complex conductivity responses

For this paper we apply the concept of c_p to our CC data. The concept of specific polarizability was first introduced by Weller et al., 2010. Evidence from previous research suggests strong dependence of specific area per unit pore volume (S_p) on CC responses for various sediments.

$$S_p = S_m \times \rho_d \times \frac{(1-n)}{n}, \quad (10)$$

where n is the porosity, ρ_d is the mineral density, and S_m is the specific surface area, which can be measured by nitrogen adsorption BET method (Brunauer et al., 1938).

Weller et al. (2010) investigated the relationship between pore-normalized specific surface area (S_p) and imaginary conductivity measured at 1Hz or normalized chargeability m_n determined from Debye decomposition for an extensive sample dataset

to establish a robust empirical model. They quantify the σ'' - S_p and m_n - S_p relationships as follows,

$$c_p = \frac{\sigma''}{S_p} \quad (11)$$

$$c_s = \frac{m_n}{S_p} \quad (12)$$

where c_p or c_s is the specific polarizability (Weller et al., 2011), and is the ratio between the imaginary conductivity or normalized chargeability, respectively, and S_p . Weller et al. (2010) discuss the concept of specific polarizability as a representation of polarization magnitude per unit pore-volume-normalized surface area, and assumed it to be determined by the chemistry and mineralogy of the polarized grain-fluid interface. Therefore, the specific polarizability concept is well suited to represent the dependence of the CC on the electrochemical factors controlling the IP responses independent of the total polarizable surface area of the sample.

Weller et al. (2010) showed the σ'' - S_p relationship fit to an extensive database of sandstone and unconsolidated sediments (Figure 5). They present strong evidence that c_p depends on clay content and mineralogy. They observe higher c_p for samples containing clay ($c_p=11.5 \times 10^{-12}$) than for sandy material ($c_p=7.2 \times 10^{-12}$). Weller et al. (2010) also observe two orders of magnitude changes in c_s for the m_n - S_p relationship for metallic samples as compared to non-metallic samples (Figure 6).

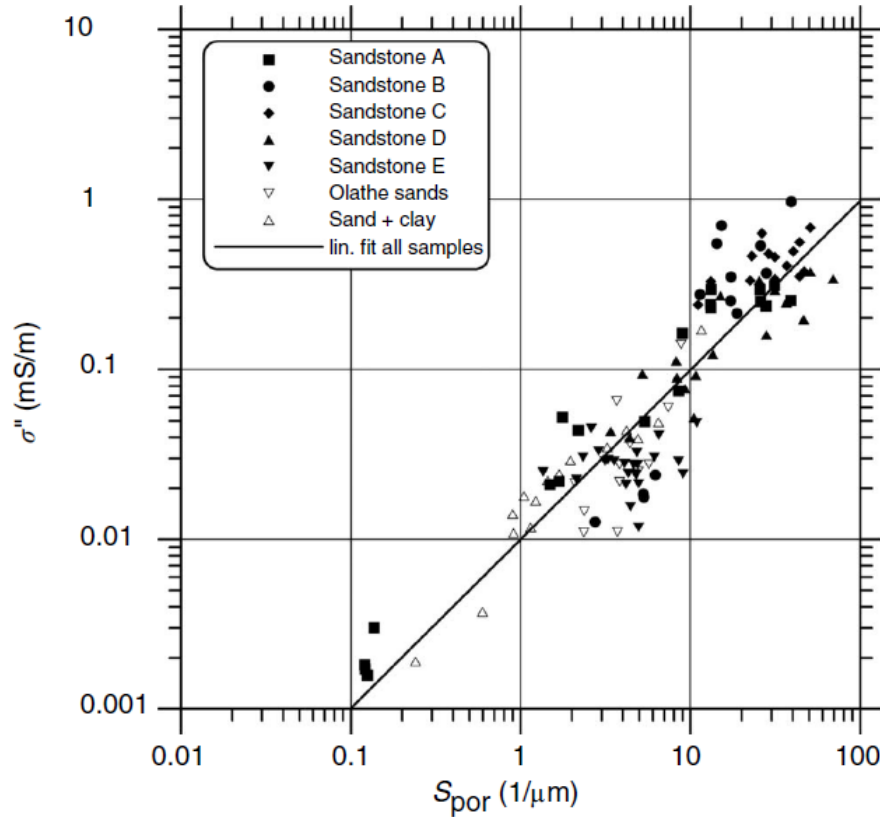


Figure 6 – Imaginary conductivity (σ'') and pore-normalized specific surface area (S_p) relation observed by Weller et al. (2010) for an extensive database of 114 samples.

To further understand the influence of salinity on the specific polarizability, Weller et al. (2012) analyze the influence of pore fluid composition on the CC responses of three different sandstones. Weller et al. (2012) observe a trend of increasing σ'' for low fluid salinity and a plateau behavior at high salinity. Similar to Lesmes and Frye (2001), Weller et al. (2012) attribute this behavior to a maximum polarizability within the measured frequency range.

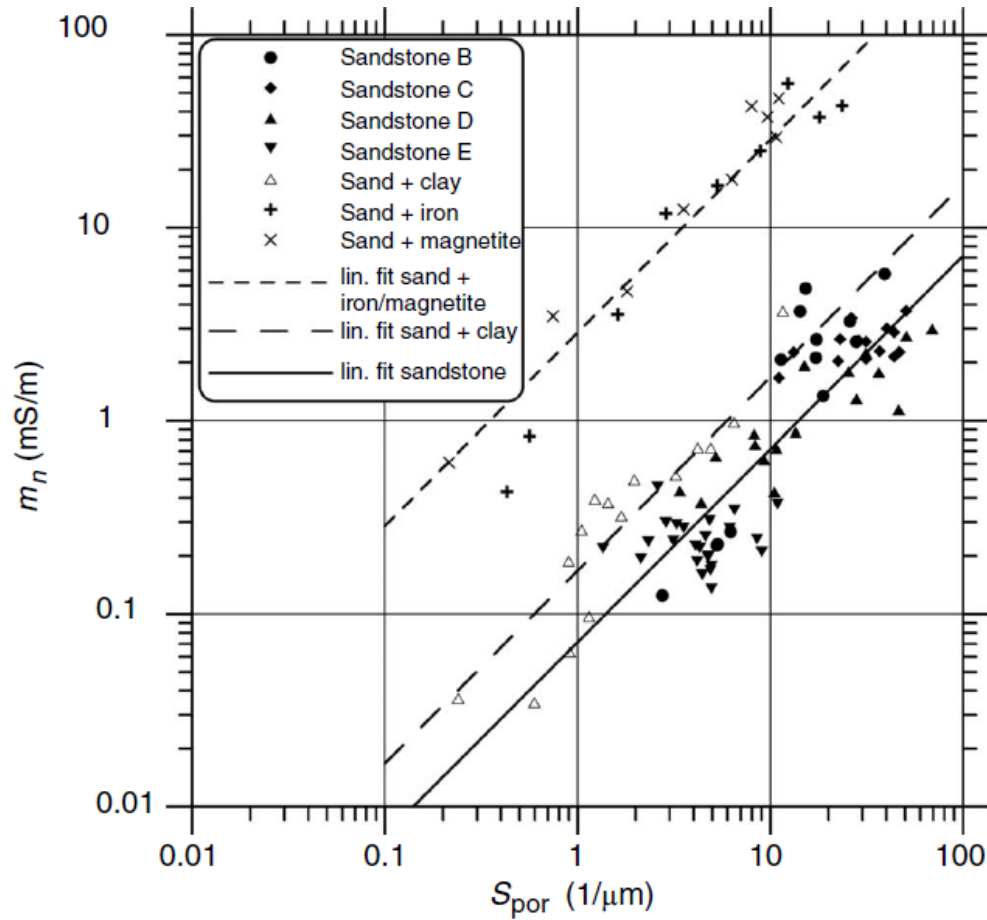


Figure 7 – Normalized chargeability (m_n) and pore-normalized specific surface area (S_p) relation observed by Weller et al (2010) for an extensive database of 114 samples. Higher c_p was observed for mixture containing clay minerals.

More recently, Weller et al. (2015) analyze a dataset consisting of 60 samples to better understand the concept of specific polarizability (c_p) (Figure 7). For their samples, they compare c_p estimates derived using S_p determined using the nitrogen gas-adsorption BET method (Brunauer et al., 1938) and wet-state methylene blue (MB) method (e.g. Yukselen and Kaya, 2008). Weller et al. (2015) observe larger S_p estimates from MB method than those obtained using the BET method, especially for the swelling clay

minerals (Figure 8). Weller et al. (2015) associate this variation in c_p estimates from BET and MB methods to the differing sensitivity of the two methods to the internal surfaces of clay minerals. The data suggest that the MB estimates of surface areas are better correlated with imaginary conductivity than the BET estimated surface areas. They come up with a single value of specific polarizability ($c_p = 7.5 \times 10^{-12}$) to describe the relationship between σ'' and S_p .

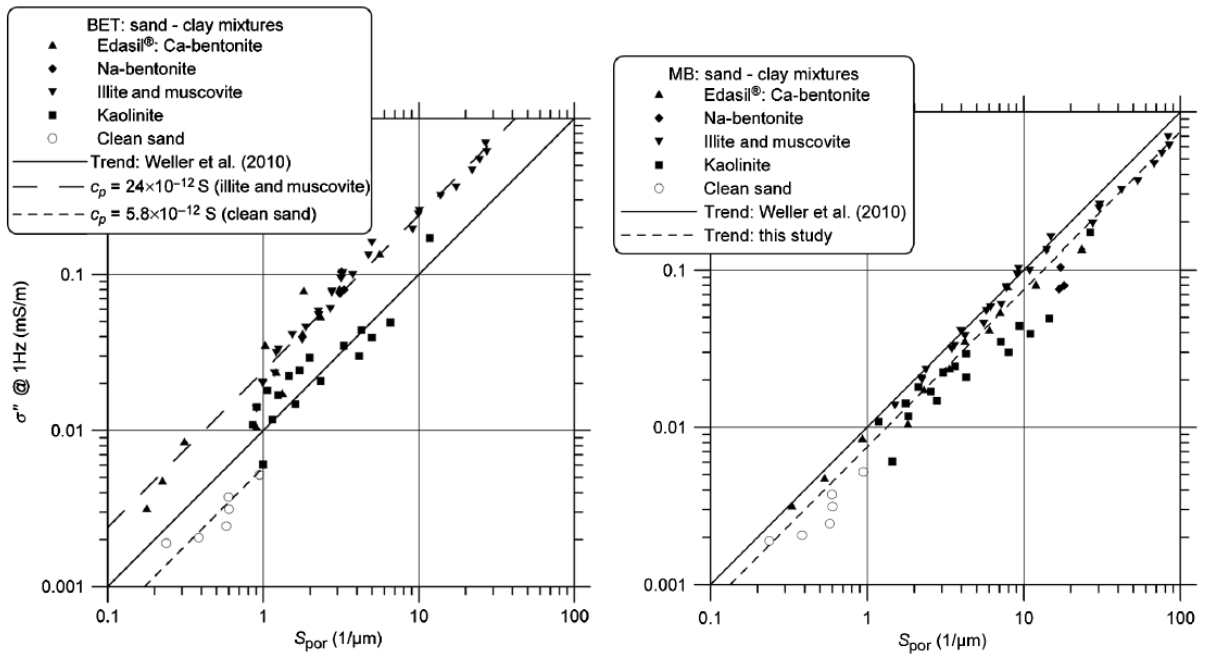


Figure 8 - Relationship between S_p (BET and MB estimates) and imaginary conductivity (σ'') observed by Weller et al. (2015).

Influence of sample saturation and clay content on imaginary conductivity

Ulrich and Slater (2004) investigated the influence of saturation on polarization measured for unsaturated, unconsolidated sediments during evaporative drying and pressure drainage followed by imbibition. For evaporative drying, sample saturation was determined by weighing samples before electrical measurements that were then dried by progressive evaporation. In order to perform pressure drainage and subsequent imbibition, a high-pressure syringe pump was used to remove and add water from the bottom of the sample holder. Sample saturation was determined using calculated sample porosity and amount of water imbibed or extracted. These measurements on unconsolidated samples confirmed that the polarization is a function of saturation. Figure 9 shows an example of imaginary conductivity spectra two for samples with the evaporative drying and pressure drainage methods, respectively. The imaginary conductivity shows a weak increase with frequency over the measured frequency range.

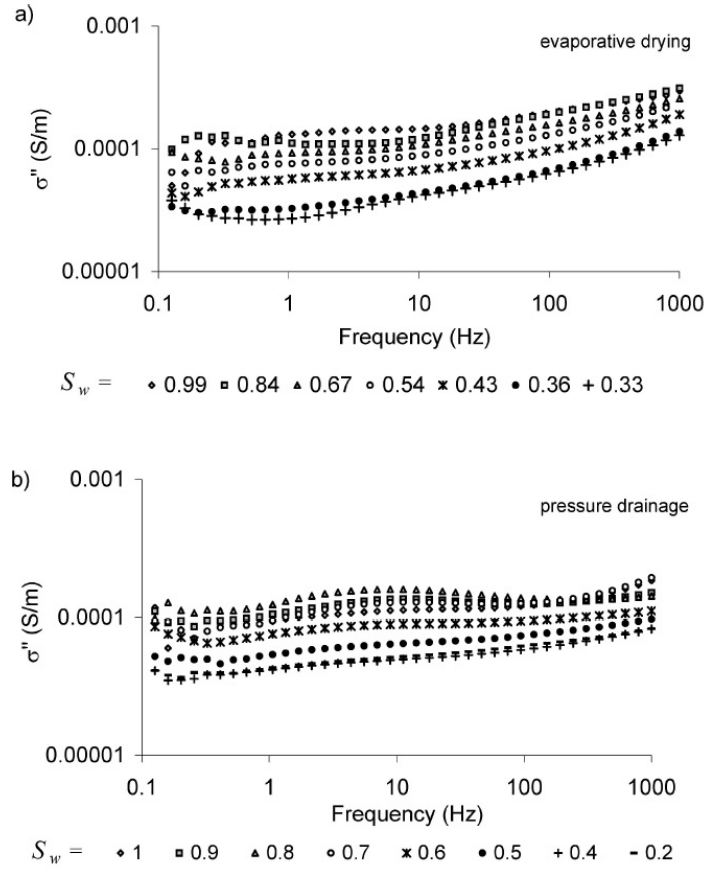


Figure 9 - Imaginary conductivity spectra as a function of saturation; a) during evaporative drying, b) during pressure drainage (Ulrich and Slater 2004).

More recently, Grunat et al, (2013) carried out experiments on an undisturbed agricultural soil to further understand the dependence of induced polarization (IP) on saturation. They observe a weak dependence of imaginary conductivity on saturation degree relative to that observed for real conductivity. Figure 10 shows a plot of imaginary conductivity vs. saturation, showing a plateau at high saturation followed by a power law decrease at lower saturation consistent with Ulrich and Slater (2004) during pressure draining.

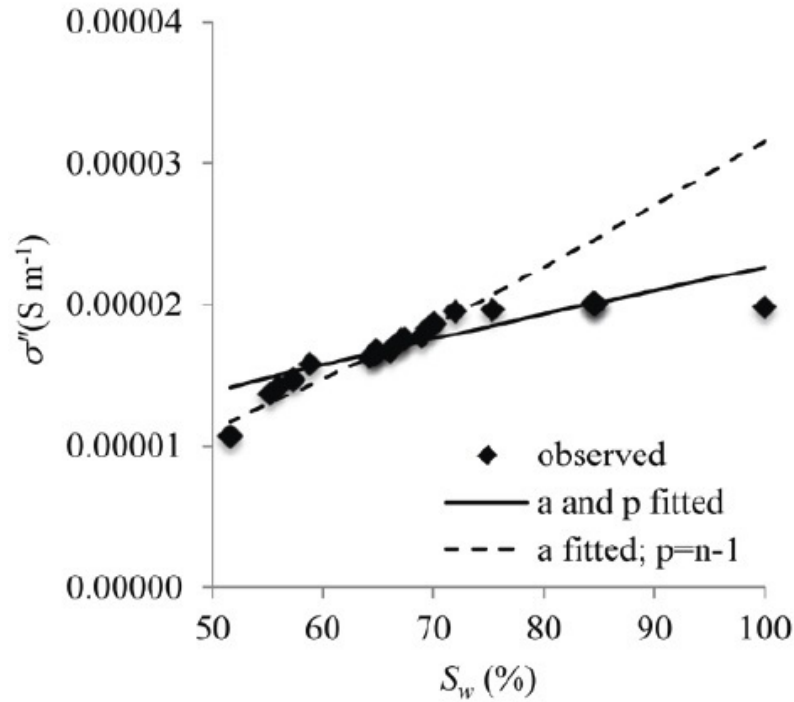


Figure 10 - Imaginary conductivity vs. percent saturation degree shows a power law relationship (Grunat et al., 2013).

Methods

Sample mixtures were prepared by carefully combining various types of clay with Ottawa sand. The mixture for kaolinite was prepared by adding 4% w/w sample to 96% w/w Ottawa sand and 2% illite mixture was prepared by adding 2% w/w sample to 98% Ottawa sand. The small clay fraction was chosen to ensure enough clay fraction within the sand matrix to allow for measurable electrical response whilst also preventing a large reduction in permeability. This procedure was similar to that adopted by Personna et al. (2013) in order to ensure consistency in experimental procedures and to permit comparison against the previous results obtained for bentonite. The nitrogen gas –

adsorption BET method (Brunauer et al., 1938) was used to determine specific surface area (S_s) of kaolinite ($9.73 \pm 0.03 \text{ m}^2/\text{g}$), illite ($34.54 \pm 0.20 \text{ m}^2/\text{g}$), bentonite ($256.76 \pm 0.45 \text{ m}^2/\text{g}$) and Ottawa sand ($0.049 \pm 0.002 \text{ m}^2/\text{g}$).

Cylindrical PVC columns were dry packed with a mixture of Ottawa sand (density (ρ) = 2.64 g/cm^3 , $d_{10} = 0.096 \text{ mm}$) and (1.) kaolinite (1:1 clay, $\rho = 2.62 \text{ g/cm}^3$, $d_{10} = 0.0010 \text{ mm}$) or (2.) illite (2:1 clay, $\rho = 2.77 \text{ g/cm}^3$, $d_{10} = 0.0013 \text{ mm}$). The PVC column schematic is summarized in Figure 11.

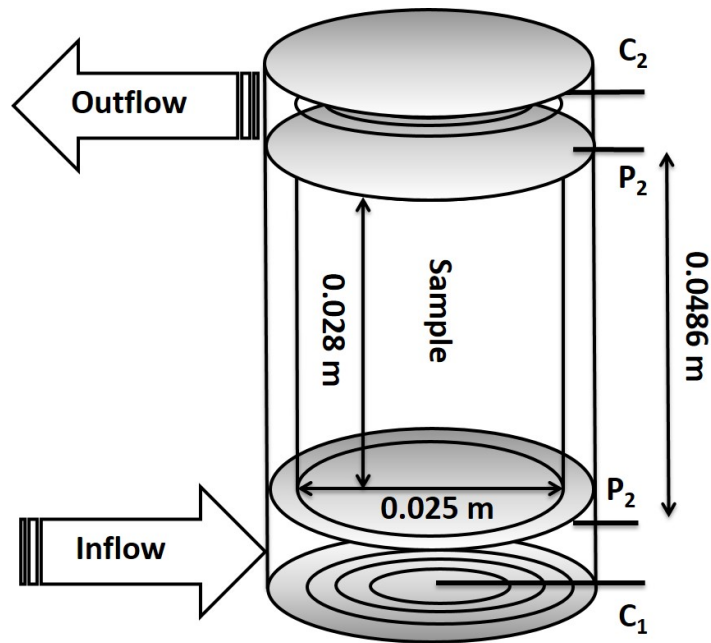


Figure 11 - Experimental setup schematic showing the sample holders constructed using cylindrical transparent PVC (inner diameter = 0.025m and length = 0.028 m). The location of two coiled Ag-AgCl current electrodes (C₁ and C₂) and two Ag-AgCl potential electrodes (P₁ and P₂) are shown.

The mixtures were then dry packed into a PVC column with a 0.45 μm cellulose membrane on either side to ensure no loss of clay during the subsequent saturation process. Also, the flow rate was kept low to ensure no redistribution of clay within the column. We found that dry packing promoted a more homogenous mixture of clay and sand and minimized redistribution of clay associated with variations in grain sizes of the clay relative to the sand mixture. The saturating fluid was either 300 $\mu\text{S}/\text{cm}$ background solution or the background solution mixed with pure ethanol (ethyl alcohol 200 proof and 99.98% assay v/v from Pharmco AAPER) in different concentrations by volume.

Personna et al. (2013) used a mixture of 2% (w/w) bentonite clay with 98% (w/w) Ottawa sand, with column packing procedures and setup identical to ours. The solution used by Personna et al. (2013) was either background water or a water-ethanol mixture made with the same pure ethanol (ethyl alcohol 200 proof and 99.98% assay v/v from Pharmco AAPER) used in our study. The water used in their experiment was well characterized, containing major ions of natural groundwater and having an electrical conductivity of 266.3 $\mu\text{S}/\text{cm}$ and comparable to the conductivity of our background solution (300 $\mu\text{S}/\text{cm}$).

The experimental treatments applied in our CC measurements are summarized in Figure 12. The kaolinite mixture contained 4% (w/w) clay with 96% (w/w) Ottawa sand. The illite and bentonite mixtures contained 2% (w/w) clay with 98% (w/w) Ottawa sand. CC measurements with 2% kaolinite were also acquired but responses were small and unreliable (see Figures A1, A2 and A3 in the appendix). This presented problems with respect to DD fitting. Therefore, it was decided to use the 4% kaolinite mixture.

Analyzing c_p (σ'' normalized by S_p) as compared to σ'' allowed the comparison of the different clay fractions together. Three different experimental treatments were applied (Figure 12) in replicate: (a) Sand-clay mixture saturated with the background solution (EtOH blank), (b) sand-clay mixture saturated with the solution containing 10% EtOH mixture (EtOH 10%, v/v) and (c) sand – clay mixture saturated with the solution containing 20% EtOH mixture (EtOH 20%, v/v). Samples were saturated with their respective saturating solutions, and placed in the same saturating fluid at the end of each measurement to allow repeated observations, which are required to monitor any temporal changes in CC response due to possible non-equilibrium effects (Personna et al. 2013).

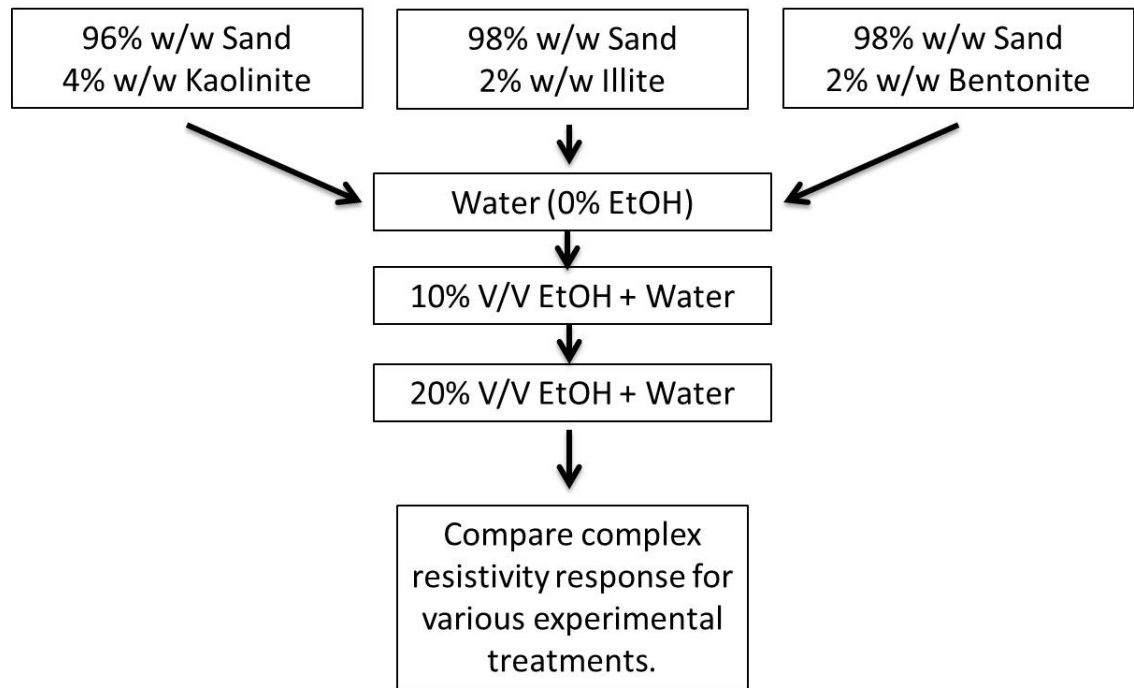


Figure 12 - Summary of experimental treatments applied to samples. We applied three experimental treatments to our samples saturated with either KCl (0% EtOH) or KCl containing 10% or 20% EtOH (v/v). Personna et al.(2013) applied a similar experimental treatment to the bentonite clay sample, with EtOH blank being water instead of KCl.

Saturation and porosity of the samples were determined from weight loss between saturated and dried samples after completion of CC measurements. Sample porosities and saturations are given in Table 1. For each sample mixture, pore volume normalized specific surface area S_p (μm^{-1}) was calculated using

$$S_p = [(Ss_x \times \rho_x \times W_x) + (Ss_{OS} \times \rho_{OS} [1 - W_x])] \times \frac{1-n}{n} \quad (15)$$

where Ss is m^2/g , n is the porosity of the mixture, W is fraction by weight, ρ is density (g/cm^3), OS refers to Ottawa sand and x refers to the clay mineral used in the mixture.

The physical characteristics of all clay minerals used are summarized in Table 1.

Table 1- Summary of measured physical properties of clay and sand-clay mixtures

Sample	D10 Particle Size (mm)	Porosity (%)	Surface Area (m^2/g)
Ottawa sand	0.6-0.7	-	0.0485 ± 0.0015
Kaolinite (1:1)	0.0010 ± 0.00011	34.3	9.7295 ± 0.0250
Illite (2:1)	0.0013 ± 0.00012	38.7	34.5386 ± 0.2002
Bentonite (2:1)	0.0030 ± 0.00010	37	256.7876 ± 0.4485
Sand-Clay Mixture	S_p (μm^{-1})	Saturation (%)	
4% Kaolin + 96% Sand	2.18 ± 0.015	96.37 ± 1.54	
2% Illite + 98% Sand	3.60 ± 0.020	88.35 ± 2.36	
2% Bentonite + 98% Sand	5.40 ± 0.010	-	

A dynamic signal analyzer (DSA) was used for all CC measurements. The conductivity magnitude ($|\sigma|$) and phase shift (ϕ) were measured relative to a reference resistor. CC measurements were acquired for 51 frequencies between 10^{-2} and 10^3 Hz and were available at 41 frequencies between 10^{-1} and 10^{-3} Hz for the bentonite sample of Personna et al. (2013). Silver-silver chloride electrodes were used for current injection as well as for recording potential measurements. The DD approach was used to fit measured CC data to compute a specific integral chargeability (m_k) and relaxation time (τ_k) to determine the CC model parameters (Equation 7, 8 and 9). Analysis of variance (ANOVA), performed with ezANOVA, was used to test the statistical significance (level of significance, $\alpha = 0.05$) of the changes in the CC data as a function of EtOH concentration.

Results

Figure 13 summarizes the specific polarizability (c_p) spectra for the three different clay-sand mixtures: 4% kaolinite, 2% illite, 2% bentonite and pure Ottawa sand. The c_p spectra shown in Figure 13 represent measurements that were taken 20-25 days after column preparation and pore fluid injection. This time elapse since sample preparation was necessary for the system to reach equilibrium. After this time, no more significant changes in specific polarizability were observed for bentonite, illite and kaolinite containing mixtures.

We observed a clear variation in the specific polarizability of the sand-clay samples as a function of clay mineralogy and increasing EtOH concentration. All sand-clay mixtures show varying degrees of changes in the specific polarizability response with increasing

EtOH concentration in the pore-filling fluid. The overall percentage suppression is similar between all three clay types (Table 2). The kaolinite mixture shows the strongest decrease in c_p with increasing EtOH concentration over the entire frequency range. On the other hand, the mixture containing bentonite shows the strongest decrease in c_s with increasing EtOH concentration. The mixture containing illite also shows suppression in specific polarizability with respect to increasing EtOH concentration across the entire frequency range. The relative changes in specific polarizability based on increasing concentration are always higher than relative changes in real part of the conductivity (spectra not shown for brevity), as summarized in Table 2.

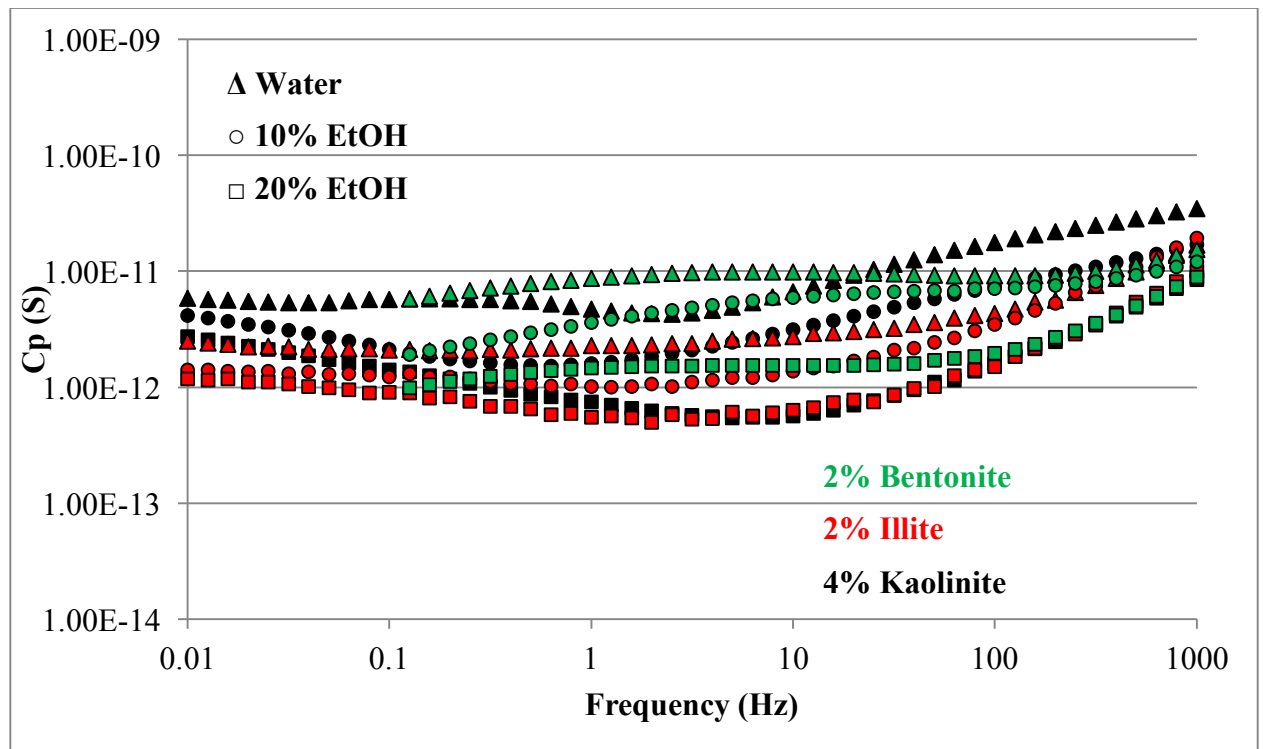


Figure 13 - Specific polarizability (c_p) responses for different clay minerals: a) bentonite (green), b) illite (red) c) kaolinite (black) and d) Ottawa sand as a function of ethanol concentration (v/v) (EtOH 0%, EtOH 10% and EtOH 20%).

The percent relative change of c_p , c_s and real conductivity were calculated based on the 10% EtOH sample as the reference is shown in Table 2. The mixture containing bentonite shows the highest relative decrease in c_s with increasing EtOH concentration followed by illite clay containing mixture. The relative changes in real conductivity for increasing EtOH concentration are much less than observed for the normalized chargeability.

However, the dependence of imaginary conductivity on the frequency complicates data interpretation for c_p . Imaginary conductivity values at different frequencies will result in a different c_p estimate (Table 2). Therefore more emphasis was placed on the variation of c_s as it is determined from normalized chargeability, which is a global estimate of polarization for the sample and is frequency independent. All three clays show varying degree of suppression in c_s responses with increasing EtOH concentration. The ANOVA for level of significance $\alpha = 0.05$ indicated that the suppression of clay-driven polarization response with increasing EtOH concentration is statistically significant, but the confidence level is low.

Table 2 – Percentage change (%) in c_p , c_s , real and imaginary conductivity. Imaginary conductivity shown for 1 Hz frequency. Negative and positive values indicate decrease or increase in c_p / c_s / real conductivity / imaginary conductivity relative to 10% EtOH sample.

Sample Mixture	c_s	c_p	σ'	σ''
	20% EtOH	20% EtOH	20% EtOH	20 % EtOH
2% Bentonite + Sand	-64.6	-73.3	12.5	-61.41
2 % Illite + Sand	-60.1	-52.7	-1.5	-45.56
4% Kaolinite + Sand	-42.9	-80.9	8.2	-53.23

Discussion

We observe clear, statistically significant variations in the clay driven polarization response for different clay – sand mixtures with increasing EtOH concentration (Figure 13). We observe suppression in c_s for all clays with increasing EtOH concentration. The polarization suppression based on c_s resulting from increasing EtOH concentration is largest in bentonite, followed by illite and least for kaolinite (Table 2). The suppression effect of EtOH on polarization for the bentonite mixtures has been previously interpreted in terms of: a) preferential adsorption of EtOH relative to water onto clay and resultant changes in clay structure, and b) complex intermolecular interactions between EtOH and water resulting in changes in mobility of ions in the EDL at the mineral surface (Personna

et al., 2013). Thus changes in specific polarizability can be attributed to geochemical alteration on clay surfaces and changes in pore-fluid chemistry which are not observed for EtOH present in pure Ottawa sand (Figure 14). The suppression could also be occurring due to the presence of silica surface, but the small phase angles recorded for silica make it undetectable with the SIP instrumentation.

Personna et al. (2013) focused on cation-dipole interactions, amongst others, to potentially explain the adsorption of EtOH on clay resulting in the alteration of surface chemistry. Similarly, suppression in clay driven polarization for illite can be explained by preferential adsorption of EtOH onto clay surfaces. However, the relative reduction in c_s with increasing ethanol concentration is comparable for all clay types (Table 2). The mixture containing bentonite shows the highest relative reduction in c_s with increasing EtOH concentration. The ANOVA for the level of significance found $\alpha = 0.05$ in that the differences between c_s values are significant for all the sand-clay mixtures, but the confidence level is low. Weller et al. (2015) show that the variation in specific surface area estimates obtained using BET and MB methods are significantly different. For our study we only had access to the dry-state BET method which only measures the external surface area, and is not capable of sensing internal surface area that also controls the magnitude of CC responses. However, the c_s data show higher suppression in bentonite clay, followed by mixtures containing illite and kaolinite. The higher polarizability of the bentonite as compared to illite and kaolinite is primarily attributed to the higher surface area.

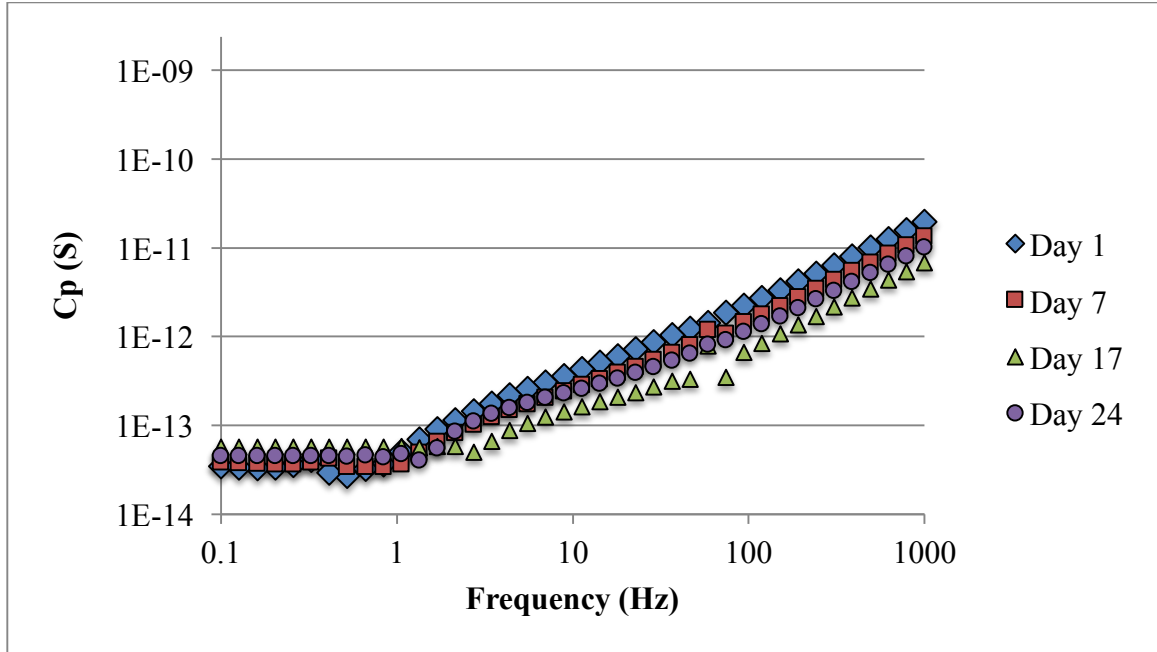


Figure 14 - Temporal variation in specific polarizability (c_p) response for Ottawa sand sample with 10% EtOH.

As shown in Table 2, the relative changes in specific polarizability (c_s and c_p) are larger than relative changes in real conductivity. This observation emphasizes the sensitivity of CC to alterations in surface geochemistry of different clay types over traditional resistivity methods where the effect of pore-fluid chemistry often dominates the surface effects. The presence of EtOH in the pore-filling fluid results in suppression of the polarization response for sand-clay mixtures, presumably due to adsorption of EtOH onto clay surfaces. The degree of adsorption is directly related to the available internal and external surface area to pore volume ratio of the mixture.

Our findings are consistent with recent studies on clay-organic interactions carried out by Personna et al. (2013) and Ustra et al. (2012). We show similar suppression in clay driven polarization for kaolinite and illite as compared to bentonite with increasing EtOH concentration. We observe greater clay-driven polarization suppression as opposed to that recorded by Ustra et al. (2012) for toluene. Ethanol, being a polar molecule, has a higher tendency for adsorption onto clay surfaces as compared to non-polar toluene. Our data reflect the variation in polarization magnitude is directly related to the internal and external specific surface area per pore volume available for adsorption. The magnitude of c_s response is a function of internal and external surfaces available for adsorption. Suppression in c_s responses is a result of the increase in EtOH concentration in the pore-filling fluid and change in clay mineralogy (Figure 15). Our data reflects the potential for CC measurement to differentiate between different types of clays at organic contaminated sites. Our findings also indicate the sensitivity of CC measurements to varying clay types and the complex kinetic and chemical ion exchange capacities for individual clay types.

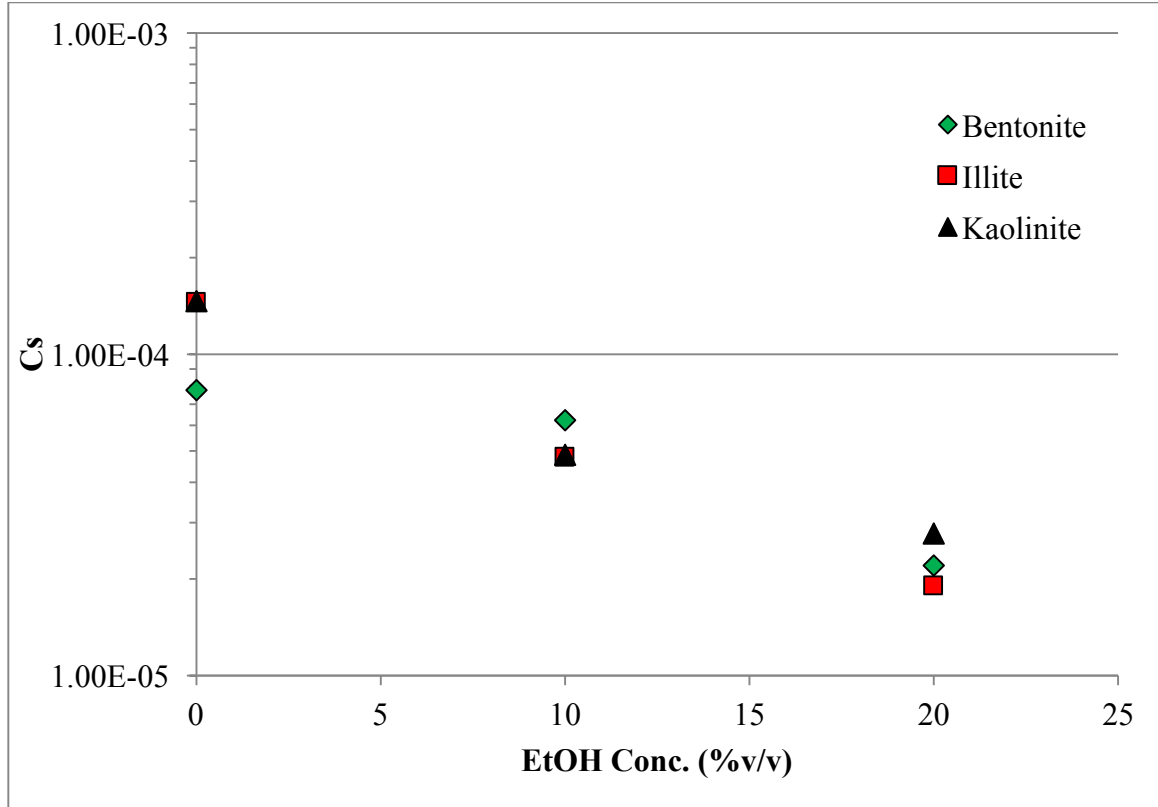


Figure 15 – Plot of specific polarizability (c_s) versus measured EtOH concentration for different sand-clay mixtures.

Conclusions

Clay-driven polarization changes are observed for both illite and kaolinite that are largely consistent with that previously observed only for bentonite (Personna et al. 2013). The c_s estimates were used to understand the effect of clay mineralogy and increasing EtOH concentration in pore-filling fluid on CC measurements. The suppression in specific polarizability in different clay mixtures as a function of EtOH is directly related to clay mineralogy and pore-fluid chemistry. The relative reduction in c_s with increasing ethanol concentration is comparable for all clay types. The mixture containing bentonite shows the highest relative reduction in c_s with increasing EtOH concentration. The smallest c_s

suppression was observed in the kaolinite samples with increasing EtOH concentration. The variations in c_s are statistically significant, but with low confidence level, and are attributed to the sensitivity of the CC method to monitor changes in the internal and external surface area for clay minerals resulting from EtOH adsorption, though the internal and external surface area were not adequately determined by the dry-state BET method. Pure sand showed no polarization response to the presence of EtOH (within the sensitivity limits of the instrumentation), supporting the hypothesis that clay-organic interactions cause the suppression effect observed in these datasets. These findings emphasize the importance of the specific polarizability concept to monitor clay-organic interaction for different clay mineralogy. The c_s estimates reflect the sensitivity of the CC measurements to investigate alteration in surface chemistry at the available surface adsorption sites (both internal and external) for different clay types resulting from various chemical ion exchange and kinetic reactions in clay-water-EtOH media. Further investigations are necessary to better relate the observed specific polarizability variations to surface reactions in mixtures containing 1:1 and 2:1 clays. In particular, more research is needed to understand the mechanism of EtOH adsorption onto different clay minerals which will lead to improved understanding of the resulting CC signatures.

References

- Atamas, N., & Atamas, A. (2009). The investigations of water-ethanol mixture by Monte Carlo method. *World Academy of Science, Engineering and Technology*, 55, 2070-3724
- Bhat, J. I., & Shetty, M. K. (2011). Evaluation of limiting molar conductance, Walden product, association constant and thermodynamic properties of sulfacetamide sodium in water+EtOH mixtures. *Journal of Molecular Liquids*, 160(3), 140–143. doi:10.1016/j.molliq.2011.03.005
- Breede, K., & Kemna, A. (2012). Spectral induced polarization measurements on variably saturated sand-clay mixtures. *Near Surface Geophysics*. doi:10.3997/1873-0604.2012048
- Cole, K.S., Cole, R.H., 1941. Dispersion and absorption in dielectrics I. Alternating current characteristics. *The Journal of Chemical Physics* 9, 341.
- Corseuil, H. X., Hunt, C. S., Ferreira dos Santos, R. C., & Alvarez, P. J. . (1998). The influence of the gasoline oxygenate ethanol on aerobic and anaerobic BTX biodegradation. *Water Research*, 32(7), 2065–2072. doi:10.1016/S0043-1354(97)00438-7
- Craig, R., F. (1974). *Craig's Soil Mechanics*. New York, NY: Spon Press
- Davidson, D., Cole, R., 1951. Dielectric relaxation in glycerol, propylene glycol, and n-propanol. *The Journal of Chemical Physics* 19, 1484.

- German, W., & Harding, D. (1969). The adsorption of aliphatic alcohols by montmorillonite and kaolinite. *Clay Miner*, 213–227.
- Gomez, D. E., & Alvarez, P. J. J. (2010). Comparing the effects of various fuel alcohols on the natural attenuation of benzene plumes using a general substrate interaction model. *Journal of contaminant hydrology*, 113(1-4), 66–76.
doi:10.1016/j.jconhyd.2010.02.002
- Grunat, D. a., Slater, L.D., Wehrer, M., 2013. Complex Electrical Measurements on an Undisturbed Soil Core: Evidence for Improved Estimation of Saturation Degree from Imaginary Conductivity. *Vadose Zo. J.* 12. doi:10.2136/vzj2013.03.0059
- Leroy, P., Revil, a, Kemna, a, Cosenza, P., & Ghorbani, a. (2008). Complex conductivity of water-saturated packs of glass beads. *Journal of Colloid and Interface Science*, 321(1), 103–17. doi:10.1016/j.jcis.2007.12.031
- Lovanh, N., Hunt, C. S., & Alvarez, P. J. J. (2002). Effect of ethanol on BTEX biodegradation kinetics: aerobic continuous culture experiments. *Water research*, 36(15), 3739–46.
- Miranda-Trevino, J. C., & Coles, C. a. (2003). Kaolinite properties, structure and influence of metal retention on pH. *Applied Clay Science*, 23(1-4), 133–139.
doi:10.1016/S0169-1317(03)00095-4
- Mortland, R. H. D. and M. M. (1967). Alcohol- Water Interactions on Montmorillonite Surfaces. I. Ethanol, (3936), 259–271.

- Okay, G., Leroy, P., Ghorbani, A., Cosenza, P., Camerlynck, C., Cabrera, J., Florsch, N., Revil, A., 2014. Spectral induced polarization of clay-sand mixtures : Experiments and modeling. *Geophysics* 79.
- Olhoeft, G. R. (1985). Low frequency electrical properties. *Geophysics*, 50(12), 2492–2503. doi:10.1190/1.1441880
- Olhoeft, G., (1986). Direct Detection of Hydrocarbon and Organic Chemicals with Ground Penetrating Radar and Complex Resistivity.
- Olhoeft, G., King, T., 1991. Mapping subsurface organic compounds noninvasively by their reactions with clays, US Geological Survey Toxic Substance Hydrology Program. Proceedings of technical meeting, Monterey, California, 552-557
- Olphen, H. v. (1977), An introduction to clay colloid chemistry, for clay technologists, geologists, and soil scientists, *John Wiley & Sons* (2nd edition).
- Österreicher-Cunha, P., Davée Guimarães, J. R., do Amaral Vargas, E., & Pais da Silva, M. I. (2007). Study of Biodegradation Processes of BTEX-ethanol Mixture in Tropical Soil. *Water, Air, and Soil Pollution*, 181(1-4), 303–317. doi:10.1007/s11270-006-9303-y
- Parke, S. a., & Birch, G. G. (1999). Solution properties of ethanol in water. *Food Chemistry*, 67(3), 241–246. doi:10.1016/S0308-8146(99)00124-7
- Pelton, S.H., Ward, S.H., Hallof, P.G., Sill, W.R., Nelson, P.H., 1978. Mineral Discrimination and Removal. *Geophysics* 43, 588–609.

- Personna, Y., & Slater, L. (2012). Electrical signatures of ethanol-liquid mixtures: implications for monitoring biofuels migration in the subsurface. *Journal of contaminant Hydrology*, 144, 79-123
- Personna, Y., & Slater, L. (2012). Electrical signatures of ethanol-liquid mixtures: implications for monitoring biofuels migration in the subsurface. *Journal of contaminant Hydrology*, 149, 76-87.
- Powers, S., & Hunt, C. (2001). The transport and fate of ethanol and BTEX in groundwater contaminated by gasohol. *Critical Reviews in Environmental Science and Technology*, 31, 79-123
- Revil, A., Karaoulis, M., Johnson, T., Kema, A. (2012). Review: Some low-frequency electrical methods for subsurface characterization and monitoring in hydrogeology. *Hydrogeology Journal*, 1-42
- Roberts, J., & Wildenschild, D. (2004). Electrical Properties of Sand–Clay Mixtures Containing Trichloroethylene and Ethanol. *Journal of Environmental & Engineering Geophysics* 9, 1.
- Ruiz-Aguilar, G. M. L., Fernandez-Sanchez, J. M., Kane, S. R., Kim, D., & Alvarez, P. J. J. (2002). Effect of ethanol and methyl-tert-butyl ether on monoaromatic hydrocarbon biodegradation: response variability for different aquifer materials under various electron-accepting conditions. *Environmental toxicology and chemistry / SETAC*, 21(12), 2631–9.

Sadowski R.M. 1988. Clay-organic interactions. MSc. Thesis. Colorado School of Mines

Schaefer, C. E., Yang, X., Pelz, O., Tsao, D. T., Streger, S. H., & Steffan, R. J. (2010).

Aerobic biodegradation of iso-butanol and ethanol and their relative effects on BTEX biodegradation in aquifer materials. *Chemosphere*, 81(9), 1104–10.

doi:10.1016/j.chemosphere.2010.09.003

Slater, L., Ntarlagiannis, D., & Wishart, D. (2006). On the relationship between induced polarization and surface area in metal-sand and clay-sand mixtures. *Geophysics*, 71(2), 1–5.

Spagnoli, G., & Fernández-Steeger, T. (2010). Potential calculation according to the Gouy and the Stern model for kaolinite and smectite. *Engineering–Hydro- ...*, 87–91. <http://doi.org/10.1474/EHEGeology.2010-13.0-07.283>

Sposito, G., Skipper, N. T., Sutton, R., Park, S., Soper, a K., & Greathouse, J. a. (1999). Surface geochemistry of the clay minerals. *Proceedings of the National Academy of Sciences of the United States of America*, 96(7), 3358–3364.

Ustra, A., Slater, L., Ntarlagiannis, D., & Elis, V. (2012). Spectral Induced Polarization (SIP) signatures of clayey soils containing toluene, 1–13. doi:10.3997/1873-0604.

van Olphen, H. (1977) An Introduction to Clay Colloid Chemistry, 2nd edition. John Wiley & Sons, New York, 57 120.

Weller, A., Slater, L., Nordsiek, S., & Ntarlagiannis, D. (2010). On the estimation of specific surface per unit pore volume from induced polarization: A robust empirical relation fits multiple data sets. *Geophysics*, 75(4).

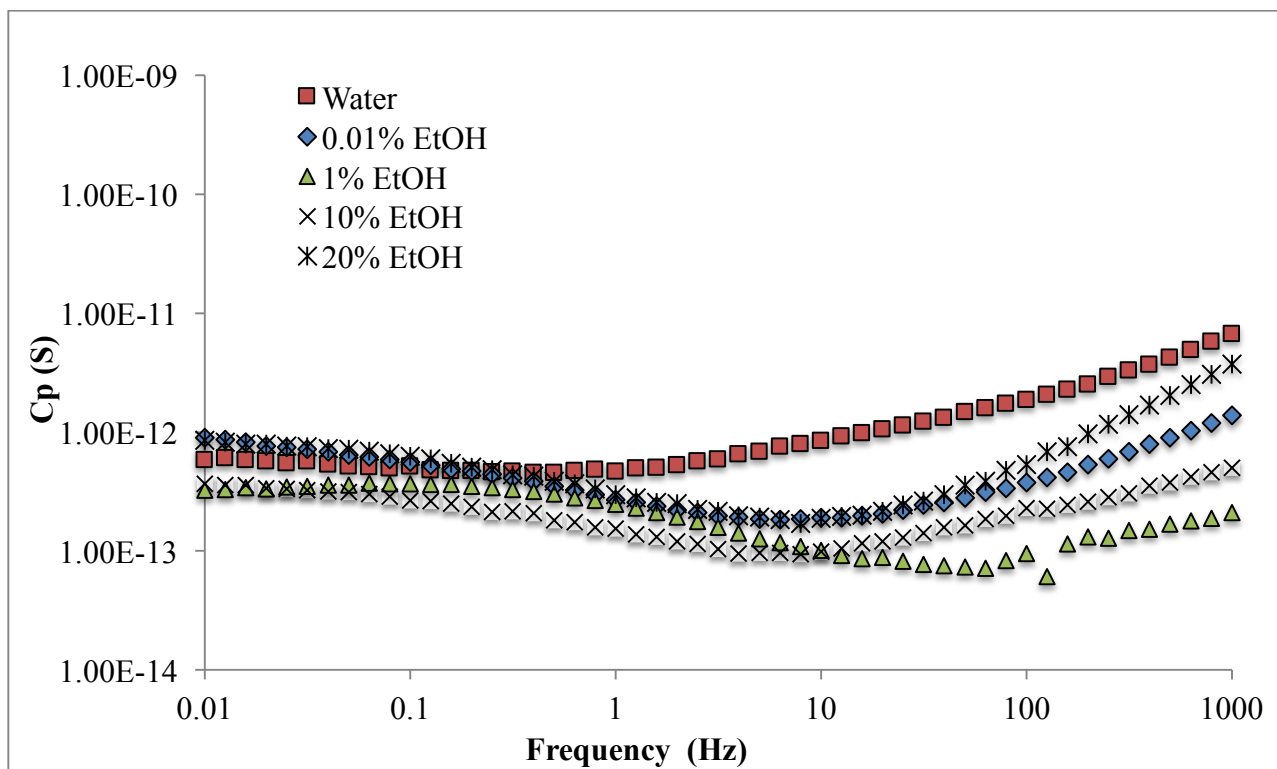
Weller, A., Breede, K., Slater, L., & Nordsiek, S. (2011). Effect of changing water salinity on complex conductivity spectra of sandstones. *Geophysics*, 76(5), F315. doi:10.1190/geo2011-0072.1

Weller, A., Slater, L., Huisman, J. A., Esser, O., & Haegel, F. (2015). On the specific polarizability of sands and sand-clay mixtures. *Geophysics*, 80(3), 3–7.

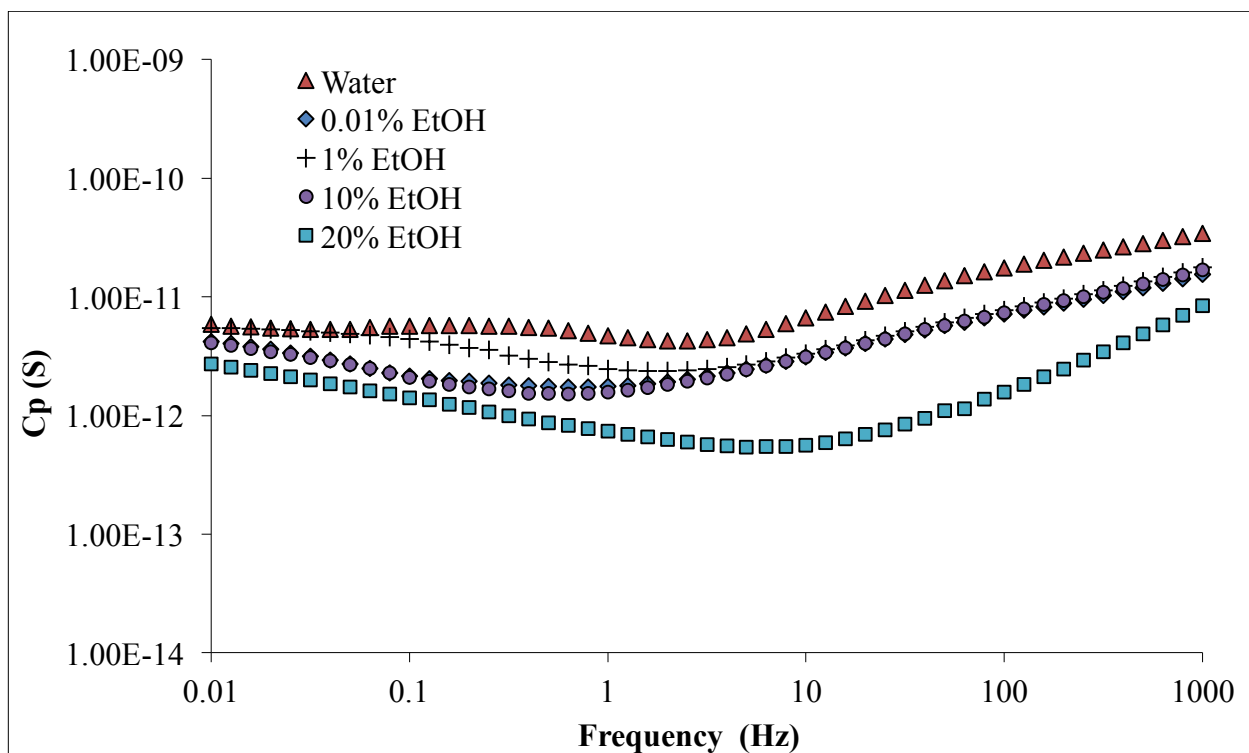
Yukselen, Y., & Kaya, A. (2008). Suitability of the methylene blue test for surface area, cation exchange capacity and swell potential determination of clayey soils. *Engineering Geology*, 102(1-2), 38–45.

Zisser, N., Kemna, A., Nover, G., 2010. Relationship between low-frequency electrical properties and hydraulic permeability of low-permeability sandstones. *Geophysics* 75, E131–E141.

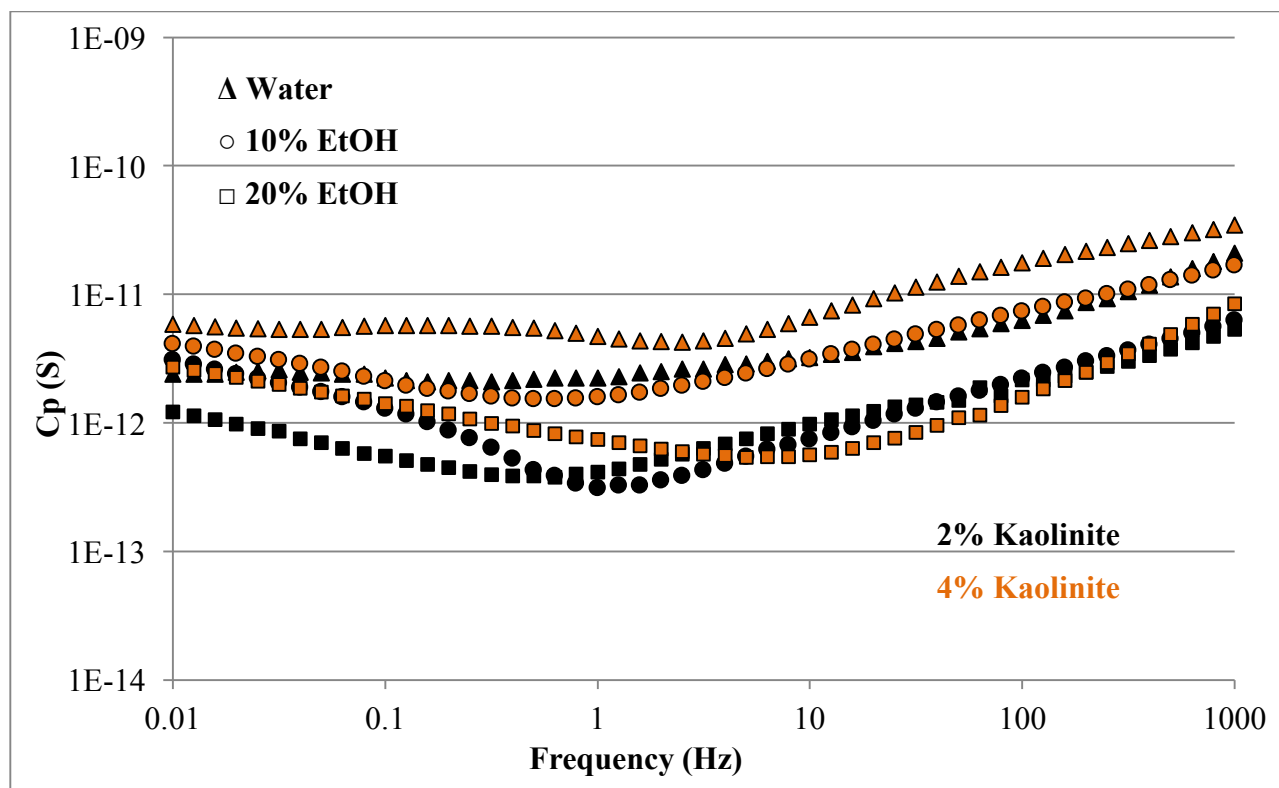
APPENDIX



Appendix A1 – Specific polarizability (C_p) of 2% kaolinite-98% sand mixture with varying ethanol concentration.



Appendix A2– Specific polarizability (C_p) for 4% kaolinite-96% sand mixture with varying ethanol concentration.



Appendix A3 – Specific polarizability (C_p) spectra for 2% and 4%- kaolinite mixture with varying ethanol concentration.